A facile one-pot green synthesis of nano-Cu$_2$O/Ca(OH)$_2$ composite by an interface reduction method

LONGFENG LI, XIAOWEN LUAN, CHEN FENG, JIAN JIANG, QINGYA YANG, MINMIN CHEN, MAOLIN ZHANG[*]

School of Chemistry and Materials Science, Huaibei Normal University, Huaibei 235000, PR China

Nano-Cu$_2$O/Ca(OH)$_2$ composites are successfully synthesized by a facile, one-pot and interface reduction method. The synthesis of these nano-composites is accomplished through the reaction of CuCl$_2$ with Ca(OH)$_2$ on its interface forming Cu(OH)$_2$/Ca(OH)$_2$ composite precursor, followed by a reduction of Cu(OH)$_2$ to Cu$_2$O with glucose as the reducing agent. The as-synthesized samples have been characterized by X-ray diffraction. The results show that the as-synthesized samples are cubic nanocrystalline Cu$_2$O/Ca(OH)$_2$ composites with Cu$_2$O average crystallite size distribution within a narrow range, indicating that the Ca(OH)$_2$ as a carrier has a controlling effect on the Cu$_2$O average crystallite size. In addition, the average crystallite size of Cu$_2$O in Cu$_2$O/Ca(OH)$_2$ composites was controlled by reaction temperature or the starting concentration of CuCl$_2$. But, reaction time has less impact on crystallinity and size of Cu$_2$O in Cu$_2$O/Ca(OH)$_2$ composites.

1. Introduction

In recent years, cuprous oxide (Cu$_2$O), a typical p-type semiconductor with a narrow band gap (ca. 2.17 eV) and a high optical absorption coefficient, has attracted increasing interest owing to its promising applications in solar cells [1], lithium-ion batteries [2], photochemical decomposition of water and organic contaminants under visible light irradiation [3-5]. Since the properties of inorganic materials vary with size, form of aggregation and dimensionality, great efforts have been devoted to the synthesis of Cu$_2$O nanoparticles with different morphologies and structures using various methods such as liquid phase reduction [6-8], hydrothermal/solvothermal synthesis [9-13], sol–gel technique [14], electrochemistry [15], chemical vapor deposition [16], chemical deposition [17] and solid state mechanochemistry [18, 19]. Compared with other synthetic methods, the liquid phase reduction that usually involves the reduction of soluble copper salts by reductants in alkaline solution, provides a more mild and flexible route for the preparation of all kinds of Cu$_2$O nanomaterials. However, the as-synthesized particles, in general, easily agglomerate in the process of liquid phase reduction. Thus, some surfactants such as Brij30 [6], polyethylene glycol [7] and octylphenyl ether [20] are added into the solution to prevent the particles aggregation and favor the growth of desired morphology. But, the addition of organic/polymer surfactants not only

increases the cost but also makes the procedure complex. In addition, residual organic/polymer surfactants probably pose the environmental risks when they are discharged into surface waters, sediments and sludge-amended soils after use [21]. Therefore, synthesis of Cu$_2$O by liquid phase reduction approach still faces the challenges.

To produce Cu$_2$O nanoparticles with narrow size distribution and uniform particle dispersion, it needs to control the homogeneity of the OH$^-$ distribution and prevent aggregation of the particles. These requirements can be met by Ca(OH)$_2$ due to its low solubility in water and the stable and homogeneous concentration of OH$^-$ in its solid-liquid interface region at a certain temperature. Herein, we report a simple, surfactant-free and environment-friendly solid interface reduction method to synthesize Cu$_2$O nanoparticles. This approach involves the reduction of Cu (II) to Cu (I) by glucose on the surface of Ca(OH)$_2$, and does not need organic additives as well as complex apparatus and techniques. Ca(OH)$_2$ serves as alkali source to provide OH$^-$, as a carrier to prevent the aggregation of Cu$_2$O nanoparticles and contribute to the separation and purification of the as-synthesized samples. In addition, we have also investigated the effects of some experimental parameters, namely, reaction temperature, reaction time, the concentration of the reactants on the crystallinity and average crystallite size of Cu$_2$O nanoparticles.

2. Experimental

All chemicals used in our experiment were of analytical grade and used without further purification. A typical procedure was as follows: 40 mL reaction mixture containing 0.1 mol/L $CuCl_2$, 0.2 mol/L glucose and 3.0 g $Ca(OH)_2$ powder was prepared in a 100 mL round-bottom flask. Subsequently, the mixture was heated at a certain temperature for a period of time under constant magnetic stirring, and then naturally cooled to ambient temperature. Finally, the as-synthesized samples were separated from the solution by filtration, sufficiently washed with distilled water, and dried in a vacuum oven at 80℃ for 6 h.

To study the effects of different experimental conditions on the crystallinity and average crystallite size of the as-synthesized Cu_2O nanoparticles, the same synthetic procedures were performed several times, changing one condition each time while the other parameters remained constant. The parameters investigated were the following: (1) reaction temperature: 60, 70, 80 and 90 °C; (2) reaction time: 0.5, 1, 2 and 4 h; (3) initial concentration of Cu^{2+}: 0.05, 0.1, 0.15 and 0.2 mol/L.

The as-synthesized samples were characterized by the X-ray powder diffractometer (A Bruker D8 ADVANCE) with Cu Kα radiation (λ= 0.15406 nm), at 40 kV and 40 mA over the 2θ degree ranging from 20° to 80°.

3. Results and discussion

The preparation of nano-Cu_2O/$Ca(OH)_2$ composite is a two-stage process. Since the solubility product constant of $Cu(OH)_2$ ($K_{sp} = 2.2 \times 10^{-20}$) is much less than that of $Ca(OH)_2$ ($K_{sp} = 4.6 \times 10^{-6}$), $Cu(OH)_2$ is firstly deposited on the surface of $Ca(OH)_2$ to form $Cu(OH)_2$/$Ca(OH)_2$ composite precursor. Subsequently, the as-prepared precursor undergoes the reduction of Cu(II) to Cu(I) by glucose, which occurs in the solid-liquid interface region of $Cu(OH)_2$/$Ca(OH)_2$, and the nano-Cu_2O/$Ca(OH)_2$ composite is obtained. These reactions can be described as follows:

$$Ca(OH)_2(s) + Cu^{2+}(aq) \xrightarrow{Precipitation\ reaction}$$
$$Cu(OH)_2/Ca(OH)_2(s) + Ca^{2+}(aq)$$
$$2Cu(OH)_2/Ca(OH)_2(s) + C_5H_{11}O_5 - CHO(aq) \xrightarrow{Reduction\ reaction}$$
$$Cu_2O/Ca(OH)_2(s) + C_5H_{11}O_5 - COOH(aq) + 2H_2O$$
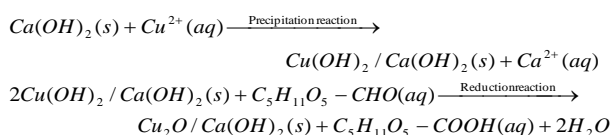
Fig. 1 shows XRD pattern of the sample synthesized at 60 ℃ for 0.5 h. The observed d-spacing values 2.463, 2.132, 1.508 and 1.283 Å, a=b=c=4.270 Å are found to match with cubic Cu_2O standard JCPDS (05-0667) data 2.465, 2.135, 1.510 and 1.287Å, a=b=c=4.268 Å, respectively. There are four peaks at 2 theta angles of 36.4°, 42.3°, 61.3° and 73.4°, indexed to (111), (200),

(220) and (311) planes of cubic Cu_2O, and the characteristic peaks of $Ca(OH)_2$ in the XRD spectrum of the synthesized sample. Moreover, the characteristic peaks of calcium carbonate ($CaCO_3$) are observed in the XRD spectra, since $Ca(OH)_2$ can absorb carbon dioxide from the air with the formation of $CaCO_3$.
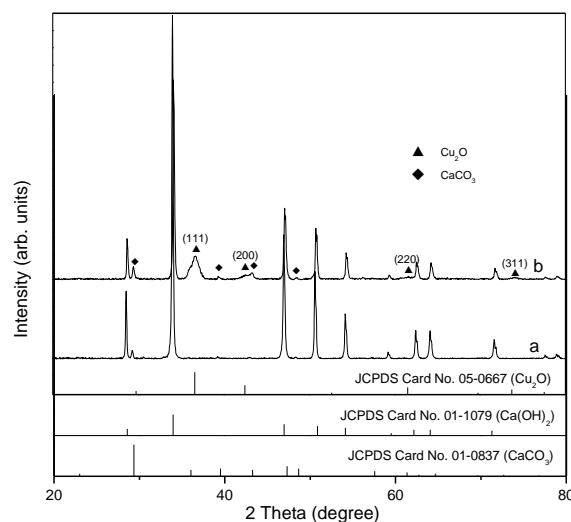
Fig. 1. XRD patterns of (a) Ca(OH)₂ raw material and (b) synthesized sample.

3.1. Effect of reaction temperature

Fig. 2 shows XRD patterns of the samples synthesized at different reaction temperatures for 0.5 h. From Fig. 2, it can be seen that the diffraction peaks intensity of Cu_2O in Cu_2O/$Ca(OH)_2$ composite gradually strengthens with the increase of reaction temperature, indicating the increase of its crystallinity. The average crystallite sizes of Cu_2O calculated from the half-value width of the diffraction peak in the (111) plane according to the Scherrer equation [22] are 13.4, 14.1, 15.3 and 16.5 nm corresponding to the reaction temperature of 60, 70, 80, 90 °C, respectively, showing the average crystallite sizes of Cu_2O increase with the increase of the reaction temperature. It can be explained as follows: the elevated temperature reduces the solubility of $Ca(OH)_2$ and the concentration of OH⁻ ion, causing the decrease in the nucleation number of $Cu(OH)_2$. In addition, the elevated temperature accelerates thermal motion of molecules. These help the growth of the $Cu(OH)_2$ precursor to get a bigger particle size, which is responsible for the change in the average crystallite sizes of Cu_2O in Cu_2O/$Ca(OH)_2$ composite with increasing temperature.
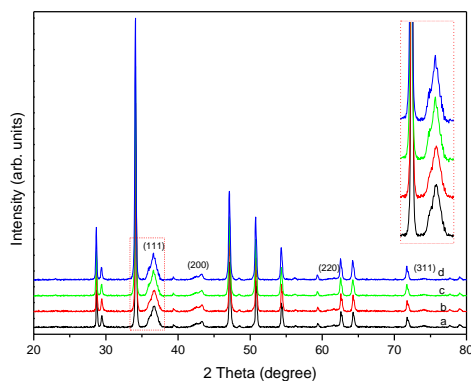
Fig. 2. XRD patterns of samples synthesized at different reaction temperature: (a) 60 ℃, (b) 70 ℃, (c) 80 ℃ and (d) 90 ℃; The inset represents the amplification of the diffraction peak in the (111) plane of Cu₂O.

3.2. Effect of reaction time

Fig. 3 shows the XRD patterns of the samples synthesized at 60 ℃ for different reaction time. As showed in Figure 3, the intensity of diffraction peaks of Cu_2O in as-synthesized $Cu_2O/Ca(OH)_2$ composite has no obvious changes as reaction time prolongs. The average crystallite sizes of Cu_2O in $Cu_2O/Ca(OH)_2$ composite are calculated from the half-value width of the diffraction peak in the (111) plane according to the Scherrer equation, with 13.4, 13.6, 13.8, 14.0 nm corresponding to the reaction time of 0.5, 1, 2, 4 h, respectively. Like the crystallinity of Cu_2O, the average crystallite sizes also have no significant changes with the extending of reaction time. This can be attributed to the following reasons: (1) the deposition of $Cu(OH)_2$ on the surface of $Ca(OH)_2$ is a fast precipitation reaction, which does not depend on the extending of reaction time under the present experimental conditions; (2) $Ca(OH)_2$ acting as a supporter can well prevent from the transfer and the growth of $Cu(OH)_2$ as well as Cu_2O nanoparticles. Therefore, the reaction time has less impact on crystallinity and size of Cu_2O in $Cu_2O/Ca(OH)_2$ composite.
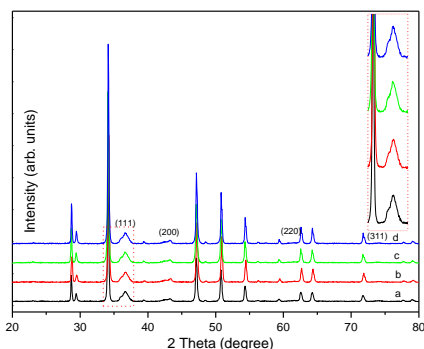
Fig. 3. XRD patterns of samples synthesized for different reaction time: (a) 0.5h, (b) 1h, (c) 2h and (d) 4h; The inset represents the amplification of the diffraction peak in the (111) plane of Cu₂O.

3.3. Effect of copper ion concentration

Fig. 4 shows the XRD patterns of the samples synthesized at 60 ℃ for 0.5h with varied initial concentration of Cu^{2+}. As showed in Figure 4, the intensity of diffraction peaks of Cu_2O in as-synthesized $Cu_2O/Ca(OH)_2$ composite significantly increases with the increase of Cu^{2+} concentration. The average crystallite sizes of Cu_2O in as-synthesized $Cu_2O/Ca(OH)_2$ composite are calculated from the half-value width of the diffraction peak in the (111) plane according to the Scherrer equation, with 15.1, 13.4, 12.3 and 11.2 nm corresponding to Cu^{2+} initial concentrations of 0.05, 0.1, 0.15, 0.2 mol/L, respectively. The results show the average crystallite sizes of Cu_2O decrease with the increase of Cu^{2+} initial concentration. This can be ascribed to the followings: As the Cu^{2+} concentration increases, the $Cu(OH)_2$ nucleation rate is higher than its crystal growth rate, causing decreasing a particle size of the $Cu(OH)_2$ precursor, which finally leads to decreasing in the average crystallite sizes of Cu_2O.
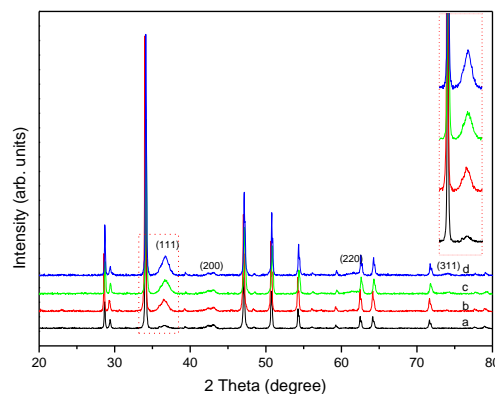
Fig. 4. XRD patterns of samples synthesized at different initial concentration of CuCl₂: (a) 0.05 mol/L, (b) 0.1 mol/L, (c) 0.15 mol/L and (d) 0.2 mol/L; The inset represents the amplification of the diffraction peak in the (111) plane of Cu₂O.

4. Conclusions

This work has developed a simple one-pot aqueous solution synthetic route for the synthesis of nano-$Cu_2O/Ca(OH)_2$ composites. The mechanism of the formation of the nano-$Cu_2O/Ca(OH)_2$ composites involves two steps: (1) the deposition of $Cu(OH)_2$ on the surface of $Ca(OH)_2$ with the formation of $Cu(OH)_2/Ca(OH)_2$ composite precursor; (2) interface reduction of $Cu(OH)_2$ to Cu_2O by glucose as the reducing agent. The as-synthesized nano-$Cu_2O/Ca(OH)_2$ composites are characterized by XRD. The results show that Cu_2O nanoparticles in $Cu_2O/Ca(OH)_2$ composites have the cubic phase structure. The average crystallite

size of Cu_2O increases with the increase of the reaction temperature and decreases with the increase of Cu^{2+} initial concentration, while reaction time has less impact on crystallinity and size of Cu_2O. In addition, Cu_2O nanoparticles in $Cu_2O/Ca(OH)_2$ composites have narrow size distribution. This is due to the control of $Ca(OH)_2$ on the migration and aggregation of Cu_2O deposited on its surface, allowing the Cu_2O nanoparticles with narrow size distribution to form.

References

[1] C. M. McShane, W. P. Siripala, K. S. Choi, J. Phys. Chem. Lett. **1**, 2666 (2010).

[2] W. Liu, G. Chen, G. He, W. Zhang, J. Nanopart. Res. **13**, 2705 (2011).

[3] Y. Yu, L. Zhang, J. Wang, Z. Yang, M. Long, N. Hu, Y. Zhang, Nanoscale Res. Lett. **7**, 347 (2012).

[4] P. Sharma, S. K. Sharma, Water Resour. Manag. **26**, 4525 (2012).

[5] M. Hara, T. Kondo, M. Komoda, S. Ikeda, K. Shinohara, A. Tanaka, J. N. Kondo, K. Domen, Chem. Commun. 357 (1998).

[6] D. Dodoo-Arhin, M. Leoni, P. Scardi, E. Garnier, A. Mittiga, Mater. Chem. Phys. **122**, 602 (2010).

[7] G. Jimenez-Cadena, E. Comini, M. Ferroni, G. Sberveglieri, Mater. Lett. **64**, 469 (2010).

[8] Z. Cheng, J. Xu, H. Zhong, X. Chu, J. Song, Mater. Lett. **65**, 1871 (2011).

[9] A. A. Al-Ghamdi, F. Al-Hazmi, O. A. Al-Hartomy, F. El-Tantawy, F. Yakuphanoglu, J. Sol-Gel Sci. Techn. **63**, 187 (2012).

[10] Y. Cui, H. Zhang, C. C. Wong, Mater. Lett. **86**, 104 (2012).

[11] S. K. Li, C. H. Li, F. Z. Huang, Y. Wang, Y. H. Shen, A. J. Xie, Q. Wu, J. Nanopart. Res. **13**, 2865 (2011).

[12] Y. Konishi, T. Nomura, D. Satoh, Ind. Eng. Chem. Res. **43**, 2088 (2004).

[13] R. Ji, W. Sun, Y. Chu, Chemphyschem **14**, 3971 (2013).

[14] A. L. Daltin, A. Addad, J. P. Chopart, J. Cryst. Growth **282**, 414 (2005).

[15] A. B. Isaev, N. A. Zakargaeva, Z. M. Aliev, Nanotech Russ. **6**, 463 (2011).

[16] H. Kobayashi, T. Nakamura, N. Takashi, Mater. Chem. Phys. **106**, 292 (2007).

[17] M. D. Susman, Y. Feldman, A. Vaskevich, I. Rubinstein, ACS Nano **8**, 162 (2014).

[18] G. R. Khayati, E. Nourafkan, G. Karimi, J. Moradgholi, Adv. Powder Technol. **24**, 301 (2013).

[19] L. Li, W. Zhang, C. Feng, X. Luan, J. Jiang, M. Zhang, Mater. Lett. **107**, 123 (2013).

[20] F. Luo, D. Wu, L. Gao, J. Cryst. Growth **285**, 534 (2005).

[21] G. G. Ying, Environ. Int. **32**, 417 (2006).

[22] B. D. Cullity, Addison-Wesley Publishing Co. Inc. 1956.

_____
*Corresponding author: mlzhang1268@163.com